EXPERIMENTAL STUDY OF 2-D ELECTROCHEMICALLY-DEPOSITED RANDOM FRACTAL MONOPOLE ANTENNAS

Christophe Dumond[1, *], Mokhtar Khelloufi[2], and Levi Allam[1]

[1]PRISME Institute, IUT of Chartres, University of Orléans, France

[2]Electronics Institute, University of Djelfa, Djelfa 17000, Algeria

Abstract—Two 2-D natural fractal monopoles generated by electro-deposition are characterized in term of measured return loss. Depending on their different shapes, previously reported multi-band behaviour and new ultra-wideband (UWB) characteristics are obtained. Finally, sufficient efficiencies are measured for both antennas proving their possible use as radiating element.

1. INTRODUCTION

Current rapid developments in telecommunication systems involve the design of antennas with multi-band/broadband behavior as well as small dimensions. As a consequence of their self-similarity and scale invariance properties, many deterministic fractal antennas with geometrical shapes have been reported to fit these requirements [1–6]. By contrast, natural fractal antennas with irregular geometry and statistical fractal dimension have not been much studied whereas fractal geometry is one of the most widespread concepts in nature. Only two previous investigations have been performed on electrochemically-deposited fractal structures. The first reports the multi-band character of an image of 2-D fractal tree printed using standard printed circuit technique [7]. The second presents the multi-band/wideband capabilities of a natural 3-D random fractal tree-monopole [8]. In this paper, a direct study of natural 2-D fractal structures generated by electro-deposition is performed. Thanks a process which has been already used to develop pollution sensors [9], an anchorage of the metallic fractal deposit is realized

on a dielectric substrate. Two real samples with different types of fractal morphologies are studied in monopole configuration. Return loss and efficiency are measured and discussed. Main advance is the achievement of UWB characteristics on this kind of natural 2-D structure. It can be noticed that a part of these results has been already presented in PIER Symposium [10].

2. RANDOM FRACTAL MONOPOLE ANTENNAS DESIGN

2.1. Structure Generation

One of the most interesting techniques to create metallic structures with random fractal shapes is electrochemical deposition. Under adequate experimental conditions, fractal morphologies could be obtained [11]. The experimental set-up used in this study, adapted from [12] consists of an electro-chemical reduction of aqueous metal ions and leads to natural solid metallic thin layer with fractal shapes supported by an insulating substrate. 2-D cells are made with 1.6 mm thick FR4 substrate on the bottom and glass plate on the top separated by thin glass spacers. Here the cell size is 11 cm × 3 cm × 0.1 mm. A 2.6 mm wide cathode (apparent on Figure 1) and an anode are etched on both edges of the upper side of the substrate while the other side is completely etched. The electrolyte solution is made of 0.02 M of copper sulfate prepared with ultra pure water. The current density being the principal drive to obtain fractal morphology, instead of constant voltages used in [7] and [8], a constant DC current is applied between electrodes in order to reach 10 to 30 $\mu A/mm^2$. An aggregation process by both diffusion and migration of the copper ions allows the growth of thin copper structures after one to five hours. It can be noticed that other fabrication techniques consisting of metallized foams have been recently used to fabricate regular fractals [13, 14].

2.2. Sample Morphologies and Antenna Design

Due to the random process used, the structures obtained are all different in size and shape but possess common fractal geometry and characteristics. While the size can be control by stopping the process, the irregular shape is randomly distributed. Therefore, depending on the constant DC current used, two main kinds of morphologies can be pointed out: lower currents lead to branched tree-like structures whereas higher currents makes the growth of planar structures with fractal contours possible. Two approximately similar in size samples with both morphologies have been chosen for
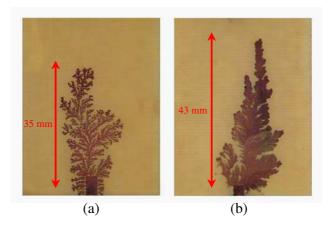
(a)   (b)

Figure 1. The studied sampler: (a) the branched tree-like structure and (b) the planar structure with fractal contour.

Table 1. Fractal dimension of sampler.

Sampler morphologie	Fractalyse 2.3	Image J	Average
Branched Tree-Like Structure	1.71	1.75	1.73
Planar Structure with Fractal Contour	1.79	1.85	1.82

investigation. A 35-mm high branched tree-like structure shown in Figure 1(a) and a 43-mm high planar structure with fractal contour shown in Figure 1(b). The fractal dimension (D) of the image of both samples have been computed by the box method using two different free software (Fractalyse 2.3 [15] and Image J$^{\text{TM}}$ [16]) and are reported in Table 1 as the average values. The fractal dimension of an object defining its capability to fill space, as expected planar structure presents higher values than branched tree-like ones. For example, the Hilbert monopole antenna presented in [17] features a fractal dimension of 2 meaning that it resembles more to a surface than to a wire.

In order to obtain monopole antenna configurations, structures of Figure 1 have been mounted vertically above a perpendicular ground plane of 0.8 mm copper thick and 20 cm × 20 cm and connected to the pin of a 3.5 mm SMA connector.

3. EXPERIMENTAL RESULTS

The input reflection coefficients S_{11} related to 50 Ω have been measured for both antennas using an HP 8720 series vector analyser. Figure 2
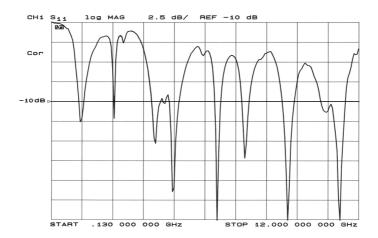
Figure 2. Return loss of the branched tree-like monopole.

Table 2. Data of the measured branched tree-like antenna.

Band (n)	Frequency F_n (GHz)	Return loss (dB)	Bandwidth VSWR < 2 (%)	Ratio F_{n+1}/F_n (−)
1	1.32	−12.6	18.9	1.95
2	2.57	−12	1.9	1.62
3	4.16	−16.5	8.6	1.16
4	4.82	−24	8.1	1.35
5	6.54	−29	3.7	1.17
6	7.62	−17	3.8	1.21
7	9.27	−25.1	5.2	1.15
8	10.68	−11.2	3.7	1.06
9	11.31	−30	4.9	-

shows the reflection coefficient of the branched tree-like monopole. The main parameters derived from the impedance matching in Figure 2 are listed in Table 2. The nine bands correspond to the S_{11} minimums of the spectrum. The resonant frequencies and their corresponding input return loss appear respectively in the second and third column. The fourth one describes the relative bandwidth for VSWR < 2 and the fifth one represents the frequency ratio between two adjacent band.

As compared to the return loss of a classical monopole of same

size, a multi-band behavior with nine apparent matching frequencies (VSWR < 2) is obtained within the measured frequency range. This multi-band character, already underlined in [7] is specific to fractal geometry and can be explained by considering fractal antennas as multiple radiating dipoles of different sizes randomly distributed in space. The complexity of the structure shape compared to conventional antennas increases the possible resonant ways for the driving currents and leads to multiple matching frequencies.

Considering the lowest resonant frequency of 1.32 GHz, the 35 mm height antenna presents an electrical size of 0.15λ. In comparison with the classic quarter wavelength resonance of a printed dipole, a shortening factor of 38.4% is obtained. This miniaturization property is one of the most reported characteristics of fractal antennas. Furthermore, the ratio between two adjacent frequencies, which is almost constant except for the first values, is also a reported specific characteristic of fractal antennas.

The return loss of the planar structure with fractal contour is presented Figure 3. Table 3 summarizes the obtained results with the five apparent resonant frequencies and their corresponding return loss in the second and third columns, the center frequency in the fourth and the bandwidth for VSWR < 2 in the fifth.

Contrary to the precedent report on this kind of 2-D structure [7] and to the tree-like monopole of Figure 1(a), the planar monopole with fractal contour of Figure 1(b) exhibits not only multi-band but
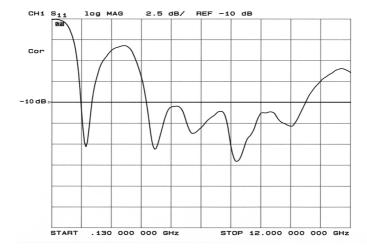

Figure 3. Return loss of the planar monopole with fractal contour.

Table 3. Data of the measured planar antenna with fractal contour.

Band (n)	Resonant frequency (GHz)	Return loss (dB)	Center frequency (GHz)	Bandwidth VSWR < 2 (GHz)
1	1.47	−15.3	1.52	1.31–1.74 (28%)
2	4.2	−15.6	7.05	3.84–10.26 (91%)
	5.81	−13.8		
	7.49	−17.1		
	9.6	−12.9		

also UWB capabilities. As it can be seen in both Figure 3 and Table 3, the fourth's last resonant frequencies merge into a single wideband that extends from 3.84 to 10.26 GHz with a fractional impedance bandwidth of 91%. Thus, the antenna appears as a dual band operating system with a second wide band which almost reaches the (3.1–10.6 GHz) band designated by the Federal Communication Commission (FCC) for UWB applications. This evolution from multi-band to wideband meets up with the result of precedent report on 3-D tree monopole [8] since our sample appears as a 2-D cut of the structure studied in [8].

As it is known for planar structures and especially for irregular fractal geometries, high current densities are concentrated close to the shape boundary. In fact, this kind of structure does not exhibit multiple discrete possible ways for the driving currents but continuous ones leading to a frequency independent behavior. The disproportion between the width and the height of the structure explains the observed rise of the return loss around 3 GHz. Considering the first matching frequency of 1.47 GHz, the antenna presents an electrical size of 0.23λ which leads to a shortening factor of 7.8% assuming a quarter wavelength resonance. The second wide band from 3.84 to 10.26 GHz can be attributed to the shape and size of the lowest part of the antenna. As suggested in current conventional study on planar UWB monopole [18], the slot between the base of the structure and the ground plane forms a traveling-wave type antenna and plays an important role in obtaining UWB characteristics. Moreover, the size of the slot opening defining approximately the lowest frequency of operation, the fractal boundary of our sample could lead to an interesting miniaturization of this kind of antenna.

Because of their thin layer characteristics, the radiation efficiency η of these antennas is an important point of interest and has also been investigated. Moreover when designing electrically small antennas the

radiation efficiency is one of the most outstanding parameters to take into account. This quantity can be expressed as the quotient:

$$\eta = \frac{P_{\text{rad}}}{P_{\text{in}}} = \frac{P_{\text{rad}}}{P_{\text{rad}} + P_{\text{loss}}} = \frac{R_{\text{rad}}}{R_{\text{rad}} + R_{\text{loss}}} \tag{1}$$

where P_{rad} is the radiated power, P_{in} is the input power, P_{loss} is the dissipated power and R_{rad} and R_{loss} are respectively the radiation and the loss resistance of the antenna.

In order to evaluate the radiation efficiencies of our antennas, the Wheeler cap method [19] and for more accuracy the post processing proposed by McKinzie [20] have been used. First, a rotation of the reflection coefficient is added until the matching frequency of interest fits the resonant frequency. The denominator of the expression (1) is then determined from the measurement of the real part of the antenna input impedance Z_{in}. Enclosing the antenna with a conducting cavity of adapted size will eliminate the radiation resistance R_{rad} from the input impedance and consequently makes it possible to determine the loss resistance R_{loss}. The radiation efficiency η of the antenna can finally be obtained by:

$$\eta = \frac{\text{Re}(Z_{\text{in}}) - \text{Re}(Z_{\text{wc}})}{\text{Re}(Z_{\text{in}})} \tag{2}$$

where Z_{in} and Z_{wc} are the measured input impedance of the antenna respectively in free space and enclosed by the cap.

Our intent is to measure the radiation efficiency of our antennas at their first matching frequencies. So that, a metallic cylindrical
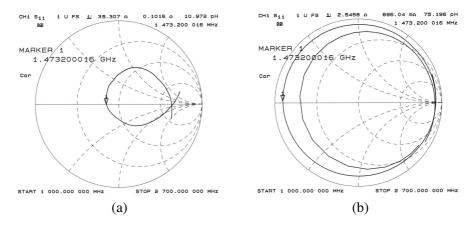

Figure 4. Input impedance Smith chart of the planar structure with fractal contour: (a) in free space and (b) enclosed by the cap.

Table 4. Efficiencies of antennas measured by McKinzie post processing of the Wheeler cap method.

Antenna under test	$R_{\mathrm{rad}} + R_{\mathrm{loss}}$ (Ω)	R_{loss} (Ω)	η (%)
Branched Tree-Like Structure	31.1	4.7	84.5
Planar Structure with Fractal Contour	35.3	2.5	92.9

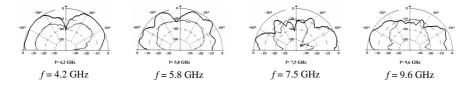$f = 4.2$ GHz $f = 5.8$ GHz $f = 7.5$ GHz $f = 9.6$ GHz

Figure 5. Radiation patterns of the planar monopole with fractal contour in the xz-plane at resonant frequencies 4.2, 5.8, 7.5, and 9.6 GHz. —— E_θ, $---$ E_φ.

cap with a radius of 50 mm, 100 mm high and 0.5 mm thick has been used. The operating frequency range is limited in low frequency by the radian length criterion and in high frequency by the emergence of first resonant mode of the cavity TM011 [21]. For our cap size, it leads to a useful frequency range from about 1 to 2.1 GHz inclosing guard-bands containing our frequencies of interest.

Figure 4 presents the Smith chart plot of the input impedance of the planar structure with fractal contour in free space and enclosed by the cap. Table 4 summarizes the results for both structures with respectively the input resistance, the ohmic losses and the resulting efficiencies. As it can be seen, the most interesting antenna in term of wideband capabilities presents also the best efficiency. Nevertheless, the sufficient efficiency achieved for both antennas demonstrate the possible use of this kind of 2-D natural fractal structures as radiating element.

To complete this study, the measured far-field radiation patterns of both E_θ and E_ϕ components for the xz-plane ($\varphi = 0$) and xy-plane ($\theta = 90$) of the planar monopole with fractal contour are presented in Figures 5 and 6 respectively for the four frequencies of interest. Each plot is normalized with respect to the maximum of the E_θ pattern and the measurement configurations are presented Figure 7. The results for the yz-plane ($\varphi = 90$) are not presented here due to their similarities with those of xz-plane.

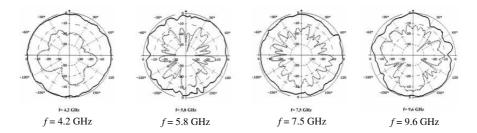Because of its elongated shape, the radiation patterns of the

f = 4.2 GHz   f = 5.8 GHz   f = 7.5 GHz   f = 9.6 GHz

Figure 6. Radiation patterns of the planar monopole with fractal contour in the xy-plane at resonant frequencies 4.2, 5.8, 7.5, and 9.6 GHz. —— E_θ, $---$ E_φ.

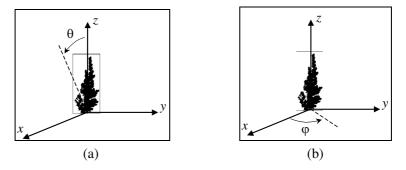(a)   (b)

Figure 7. Measurement configuration in (a) xz-plane, $\varphi = 0$ and (b) xy-plane, $\theta = 90$.

antenna fit approximately those of a printed thick monopole for all resonant frequencies. All along the xz-plane throughout the bands, classic two-lobes behaviors are obtained with a pronounced null around $\theta = 0$ except for $f = 9.6$ GHz. Also, for $f = 5.8$ and 7.5 GHz, the E_θ patterns present some additional dips. As discussed before, for planar fractal structure, high current densities are concentrated closed to the shape boundary. So all of these degradations in the radiation patterns could be linked to the excitation of higher order modes in the resonance mechanism of the structure. Similar observations can be done on the xy-plane patterns. For the three highest frequencies, the E_θ components present some irregularities compared to an isotope behavior as well as the E_ϕ components present an increasing number of ripples. These kinds of results are characteristic of fractal antennas. It can finally be noticed that for all patterns, the cross-polarization (E_ϕ) is around 10 dB less than the co-polarization (E_θ).

4. CONCLUSION

Two 2-D electrochemically-deposited random fractal monopoles with different morphologies have been presented and studied. For the first time, investigations have been done directly on natural structures. The branched tree-like structure with a fractal dimension of 1.73 is very interesting from a miniaturization point of vu with an electrical size of 0.15λ for its first matching frequency. This leads to a shortening factor of 34.8% assuming a quarter-wavelength resonance. In term of return loss, this sample presents a multi-band behavior already pointed out by a previous study on this topic [8]. By contrast, the planar structure with fractal contour fills more completely the 2-D surface with a fractal dimension of 1.82 but is less interesting in term of miniaturization with an electrical size of 0.23λ for its first matching frequency. However, its return loss exhibits original and novel UWB capabilities never reported before for natural 2-D fractal antennas. These broadband characteristics can be linked to higher fractal dimension and attributed to the shape of the opening slot between ground plane and antenna. Additionally, sufficient efficiencies of respectively 84.5 and 92.9% have been measured confirming their possible use as radiating element. Finally, far-field radiation patterns measurements have been performed on the branched tree-like structure. The results show that the fractal monopole behaves around like a printed monopole antenna for all frequencies of interest.

Main conclusion of the study is to highlight the usefulness of natural fractal shape for the design of UWB antennas. In fact, a random shape whose return loss fits perfectly the needs of a particular wireless standard could be the best solution in term of antenna miniaturization. Obviously, the random nature of electro-deposition involves a difficulty in the antenna's reproducibility. Two ways can be explored in the future: firstly, the elaboration of a fabrication process which includes measurements and automatically stops when a standard is reached. Secondly, investigations should be done on image of samples realized by classical printed circuit technique. Thanks to that, additional configurations such as feeder of planar slot or as planar monopole could be tested.

ACKNOWLEDGMENT

REFERENCES

1. Puente, C., J. Romeu, R. Pous, and A. Cardama, "On the behaviour of the Sierpinski multi-band fractal antenna," *IEEE Transactions on Antennas and Propagation*, Vol. 46, No. 4, 517–524, Apr. 1998.

2. Xu, L. and M. Y. W. Chia, "Multi-band characteristics of two fractal antennas," *Microwave and Optical Technology Letters*, Vol. 23, No. 4, 242–245, Nov. 1999.

3. Werner, D. H., A. R. Bretones, and B. R. Long, "Radiation characteristics of thin-wire ternary fractal trees," *IEE Electron. Lett.*, Vol. 35, No. 8, 609–610, Apr. 1999.

4. Puente, C., J. Romeu, and A. Cardama, "The Koch monopole: A small fractal antenna," *IEEE Transactions on Antennas and Propagation*, Vol. 48, No. 11, 1773–1781, Nov. 2000.

5. Anguera, J., C. Puente, C. Borja, and J. Soler, "Fractal-shaped antennas: A review," *Wiley Encyclopedia of RF and Microwave Engineering*, Vol. 2, 1620–1635, 2005.

6. Anguera, J., E. Martínez, C. Puente, C. Borja, and J. Soler, "Broadband dual-frequency microstrip patch antenna with modified Sierpinski fractal geometry," *IEEE Transactions on Antennas and Propagation*, Vol. 52, No. 1, 66–73, Jan. 2004.

7. Puente, C., J. Claret, F. Sagués, J. Romeu, M. Q. Lopez-Salvans, and R. Pous, "Multi-band properties of a fractal tree antenna generated by electrochemical deposition," *IEE Electron. Lett.*, Vol. 32, No. 25, 2298–2299, Dec. 1996.

8. Rmili, H., O. Mrabet, J. M. Floch, and J. L. Miane, "Study of an electrochemically-deposed 3D-fractal tree-monopole antenna," *IEEE Transactions on Antennas and Propagation*, Vol. 55, No. 4, 1045–1050, Apr. 2007.

9. Allam, L., T. Devers, and V. Fleury, "Capteurs de molécules réducrices," brevet CNRS/Université d'Orléans, FR00/10147, 2000.

10. Dumond, C., M. Khelloufi, and L. Allam, "Multiband and ultrawideband properties of 2-D electrochemically-deposited random fractal monopole antennas," *PIERS Proceedings*, 850–851, Marrakesh, Morocco, Mar. 20–23, 2011.

11. Trigueros, P. P., J. Claret, F. Mas, and F. Sagués, "Pattern morphologies in zinc electro-deposition," *J. Electroanal. Chem.*, Vol. 312, 219–235, 1991.

12. Fleury, V., W. A. Watters, L. Allam, and T. Devers, "Rapid galvanic electroplating of insulators," *Nature*, Vol. 416, 716–719,

2002.

13. Anguera, J., J. P. Daniel, C. Borja, J. Mumbrú, C. Puente, T. Leduc, N. Laeveren, and P. van Roy, "Metallized foams for fractal-shaped microstrip antennas," *IEEE Antennas and Propagation Magazine*, Vol. 50, No. 6, 20–38, Dec. 2008.

14. Anguera, J., J. P. Daniel, C. Borja, J. Mumbru, C. Puente, T. Leduc, K. Sayegrih, and P. van Roy, "Metallized foams for antenna design: Application to fractal-shaped Sierpinski-Carpet monopole," *Progress In Electromagnetics Research*, Vol. 104, 239–251, 2010.

15. Fractalyse 2.3, Laboratoire ThéMa (CNRS — Université de Franche-Comté), http://www.fractalyse.org.

16. Image J^{TM}, Java image processing program inspired by NIH Image, http://rsbweb.nih.gov/ij/.

17. Anguera, J., C. Puente, E. Martínez, and E. Rozan, "The fractal Hilbert monopole: A two-dimensional wire," *Microwave and Optical Technology Letters*, Vol. 36, No. 2, 102–104, Jan. 2003.

18. Abosh, A. M. and M. E. Bialkowski, "Design of ultra-wideband planar monopole antennas of circular and elliptical shape," *IEEE Transactions on Antennas and Propagation*, Vol. 56, No. 1, 17–23, Jan. 2008.

19. Wheeler, H. A., "The radian-sphere around a small antenna," *Proc. IRE*, 1325–1331, Aug. 1959.

20. McKinzie, III, W. E., "A modified Wheeler cap method for measuring antenna efficiency," *IEEE International Symposium on Antennas and Propagation*, Vol. 1, 542–545, 1997.

21. Austin, B. A., "Resonant mode limitations with the Wheeler method of radiation efficiency measurement," *IEE Colloquium on Advances in the Direct Measurement of Antenna Radiation Characteristics in Indoor Environments*, 7/1–7/4, 1989.